OPEN ACCESS

UNIVERSITY OF THE WEST of SCOTLAND
UWS

UWS Academic Portal

“Pipe Organ” inspired air-coupled ultrasonic transducers with broader bandwidth

Zhu, B.; Tiller, B.; Walker, A.J.; Mulholland, A.J.; Windmill, J.F.C.

Published in:
IEEE Transactions on Ultrasonics, Ferroelectrics, and Frequency Control

DOI:
10.1109/TUFFC.2018.2861575

E-pub ahead of print: 31/07/2018

Document Version
Peer reviewed version

Link to publication on the UWS Academic Portal

Citation for published version (APA):
Zhu, B., Tiller, B., Walker, A. J., Mulholland, A. J., & Windmill, J. F. C. (2018). “Pipe Organ” inspired air-coupled ultrasonic transducers with broader bandwidth. *IEEE Transactions on Ultrasonics, Ferroelectrics, and Frequency Control*, *65*(10), 1873-1881. https://doi.org/10.1109/TUFFC.2018.2861575

General rights
Copyright and moral rights for the publications made accessible in the UWS Academic Portal are retained by the authors and/or other copyright owners and it is a condition of accessing publications that users recognise and abide by the legal requirements associated with these rights.

Take down policy
If you believe that this document breaches copyright please contact pure@uws.ac.uk providing details, and we will remove access to the work immediately and investigate your claim.

Download date: 05 May 2023

“© © 2018 IEEE. Personal use of this material is permitted. Permission from IEEE must be obtained for all other uses, in any current or future media, including reprinting/republishing this material for advertising or promotional purposes, creating new collective works, for resale or redistribution to servers or lists, or reuse of any copyrighted component of this work in other works.”

“Pipe Organ” Inspired Air-coupled Ultrasonic Transducers with Broader Bandwidth

B. Zhu, *Student Member, IEEE*, B. Tiller, A. J. Walker, A. J. Mulholland and J. F. C. Windmill, *Senior Member, IEEE*

***Abstract*—Piezoelectric micromachined ultrasonic transducers (PMUTs) are used to receive and transmit ultrasonic signals in industrial and biomedical applications. This type of transducer can be miniaturized and integrated with electronic systems since each element is small and the power requirements are low. The bandwidth of the PMUT may be narrow in some conventional designs, however it is possible to apply modified structures to enhance this. This paper presents a methodology for improving the bandwidth of air-coupled PMUTs without sensitivity loss by connecting a number of resonating pipes of various length to a cavity. A prototype piezoelectric diaphragm ultrasonic transducer is presented to prove the theory. This novel device was fabricated by additive manufacturing (3D printing), and consists of a PVDF thin film over a stereolithography designed backplate. The backplate design is inspired by a pipe organ musical instrument, where the resonant frequency (pitch) of each pipe is mainly determined by its length. The -6dB bandwidth of the “pipe organ” air-coupled transducer is 55.7% and 58.5% in transmitting and receiving modes, respectively, which is ~5 times wider than a custom-built standard device.**

Keywords—Air-Coupled Ultrasound; Broad Bandwidth; Additive manufacture; 3D Print; PVDF; Piezoelectric Diaphragm Ultrasonic Transducer

I. Introduction

Higher resolution is the one of the most important requirements in non-destructive evaluation (NDE), biomedical imaging and underwater sonar [1]. A broad bandwidth ultrasonic probe can achieve this requirement because the pulse width in the time domain is shorter when the bandwidth is wider. Piezoelectric composite transducers can have wide bandwidths by optimizing their electrical and mechanical properties [1], [2]. However, the composite transducer has much better performance in water compared to air because the acoustic impedance of the composite piezoelectric material is closer to that of water. A solution to this is to add matching layers or damping materials to broaden the frequency response around resonances [2]. However, this will also decrease the device’s sensitivity. Whereas the piezoelectric transducers use thickness mode resonances, the micromachined ultrasonic transducers (MUTs) have a thin flexible film to transmit and receive ultrasound. MUTs have better performance in air because the flexible film is easier to couple with the media, with a more closely matched mechanical impedance. Further, as the film stores much less kinetic energy than bulk piezo ceramic, the MUTs have larger bandwidths when in resonance [2]. The MUTs’ family includes piezoelectric micromachined ultrasonic transducers (PMUTs) and capacitive micromachined ultrasonic transducer (CMUTs). Both of these device designs have the same flexure thin film and rigid backplate structure as shown in Figure 1(a). The flexure vibrations of CMUTs are caused by an electrostatic force generated from an electric field between the conducting backplate and metalized film. The deflection of the PMUTs’ membrane is caused by lateral strain generated from the piezoelectric effect of its piezoelectric layer [3]. The different vibration mechanism provides PMUTs with a larger transmission sensitivity, and furthermore no bias voltage is required [3], [4]. However, the bandwidth of conventional PMUTs are narrow [3],[4],[5], thus making them unsuitable for wide bandwidth applications [6],[7]. A PMUT’s bandwidth can be broadened by applying some modified structures [3],[8], such as overlapping and arranging the frequency spectrum of membranes of different size and shape [9], or using rectangular membranes [6].

The pipe organ backplate proposed in this paper is a novel design that can improve the bandwidth of air-coupled PMUTs without sensitivity loss or increase of active area. The concept and the mathematical model was proposed by Walker and Mulholland [10]–[12] and the principle was validated via prototyping [13],[14].

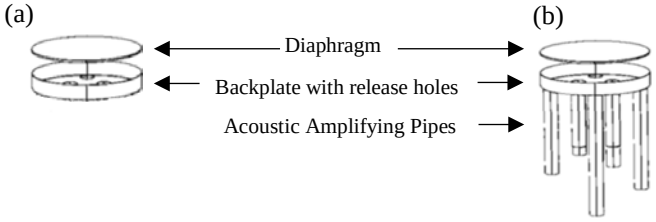

Figure 1. (a) Conventional MUT, (b) Pipe organ piezoelectric diaphragm ultrasonic transducer.

The next section describes the theoretical background of the pipe organ backplate. Section 3 uses a FEA model to simulate the device and explain the resonant frequencies created from the backplate. Section 4 introduces the manufacturing technique for the stereolithography pipe organ backplate, an improved resin formula, and the rest of the fabrication steps of the prototypes using the stereolithography backplate and commercial polyvinylidene fluoride (PVDF) thin film. Section 5 shows the experiment results of the prototypes, and the article is then discussed and concluded in Section 6.

B. Zhu, B. Tiller and J.F.C. Windmill are members of the Centre for Ultrasonic Engineering, Electronic and Electrical Engineering Department, University of Strathclyde, Glasgow, Scotland, UK, G1 1XW (e-mail: {botong.zhu, benjamin.tiller, james.windmill} @strath.ac.uk).

A. J. Mulholland is a member of the Department of Mathematics and statistics, University of Strathclyde, Glasgow, Scotland, UK, G1 1XH (e-mail: anthony.mulholland @strath.ac.uk).

A. J. Walker is a member of the School of Science and Sport, University of the West of Scotland, Paisley, UK, PA1 2BE (e-mail: Alan.Walker@uws.ac.uk).

II. Theoretical Background

A PMUT utilizes a piezoelectric layer on the top of a silicon membrane and operates in a flexural mode. After applying an electrical field to the thin plate, the lateral strain in its thickness direction makes the structure bend [15]. The vibrating membrane compresses the air and produces ultrasound. In contrast, the received ultrasound wave vibrates the film which causes charge migration between the two electrodes on the piezoelectric layer, which then can be detected by a receiving circuit [15]. The intrinsic stress of the thin plate is the factor that can dominate the resonant frequency of transducer. When the transducer has an edge-clamped film with low intrinsic stress, the resonant frequency of the circular thin plate (f_{tp}) can be estimated by equations (1) and (2) [3], where n is the number of the resonance mode, R is the radius of the thin plate, D_E is the flexural rigidity of the circular thin plate, h is the height of the cavity, ρ is the density of the thin plate, E is the Young's modulus and μ is the Poisson ratio. The squeeze film effect occurs when the air gap (depth of cavity) is very narrow [16]. Squeeze film damping becomes more important than the drag force damping of air if the thickness of the gas film is smaller than one-third of the width of the plate [16]. However, this effect can be ignored in the pipe organ design presented here because the air gap is four times higher than the thickness of the thin plate. Moreover, the change of the gap depth introduced by the vibration of the thin plate is always less than 1% of the depth of the gap.

$$f_{tp} = \frac{n}{2\pi R^2}\sqrt{\frac{D_E}{\rho h}} \tag{1}$$

$$D_E = \frac{Eh^3}{12(1-\mu^2)} \tag{2}$$

A pipe organ produces sound by driving pressurized air into each individual pipe via the keyboard and pump system. The shape of individual pipes affects the sound produced, however, the resonant frequencies of the pipes are mainly determined by the length of the pipes and the velocity of sound [12]. The resonant frequency can be calculated by the theory of pipes [13] which states that the fundamental resonant frequency of an open pipe (both ends open) occurs when the length of pipe is equal to $\lambda/2$, where λ is the wavelength of sound, and the fundamental resonant frequency of a closed pipe (one end is closed and the other end is open) occurs when the length of pipe is equal to $\lambda/4$. The resonant frequency of open cylindrical pipes is given by equation (3), where v is the speed of sound in air, L is the length of pipe and r is radius of the pipe.

$$f_p = \frac{nv}{2(L+1.6r)} \tag{3}$$

The pipes connecting the cavity to the atmosphere enable air to flow in and out which can further reduce the effect of squeeze film damping and squeeze film resistance.

A Helmholtz resonator is an air-filled cavity with one open end. When a sound wave gives an initial force to a portion of air (depicted as the grey part in Figure 2), the air will vibrate since the air inside the cavity acts as a spring. Therefore, the Helmholtz resonator can be regarded as a very classic spring-mass system that can support harmonic motion. In the pipe organ backplate, the pipes and cavity are formed into a Helmholtz resonator [17]. Similar to the organ pipes with different length and resonant frequencies, this resonator also has a resonant frequency (f_h) that can improve the sensitivity in a specific frequency range. The central frequency can be calculated by equation (4), where S is the total cross-sectional area of the pipe, and V is the volume of the cavity.

$$f_h = \frac{v}{2\pi}\sqrt{\frac{S}{VL}} \tag{4}$$

Helmholtz resonators are well-documented in many acoustic applications including acoustic energy harvesters [18], [19] and MEMS microphones [20], where they are used to enhance the sensitivity when receiving sound. The pipe organ diaphragm ultrasonic transducer proposed in this paper is based on the conventional MUTs design (as in Figure 1(a)), but connects many acoustic amplifying pipes with different lengths to the backplate (as in Figure 1(b)) to enhance the bandwidth in both transmitting and receiving modes. The design stage involves optimizing each pipe's length, and the cavity's size, so their resonant frequencies are close but not equal to the thin plate's resonant frequency and in so doing the overall bandwidth is increased. Moreover, the pipe-organ inspired resonator can amplify selected frequencies in receiving and transmitting ultrasound. As shown in Figure 3, the metalized PVDF layer is clamped on the top of the backplate as an active part to produce (or receive) ultrasound and the pipe organ backplate can be thought of as a "musical instrument" which can amplify different selected frequencies (pitches) at the same time.

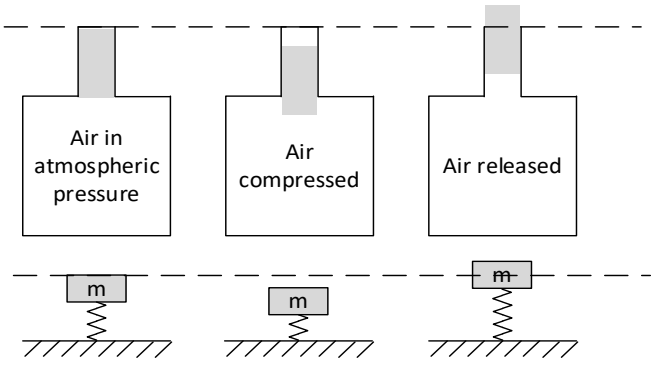

Figure 2. Schematic of a Helmholtz Resonator

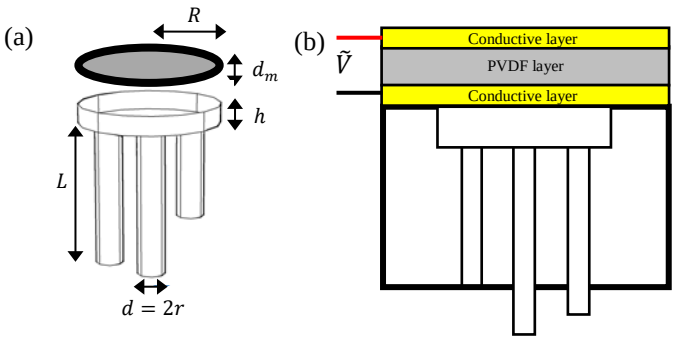

Figure 3. (a) Parameters of the pipe organ transducer (b) Sectional-cut plot of the backplate and the piezoelectric membrane

III. Finite Element Modelling

Walker and Mulholland investigated the relationship between the number of pipes and the bandwidth improvement of the pipe organ transducers through 1D mathematical models [10]–[12]. They concluded that the bandwidth increased as the number of pipes increased, up to a perceived limit when over 80 pipes were used. In this present work, there were manufacturing constraints and so the study investigated devices with no pipes, 4 pipes, 8 pipes and 13 pipes emerging from the back cavity. The effect of the orientation of pipes on the performance of the transducers was also investigated.

Figure 4(a) is a schematic of the pipe organ transducer which was simulated by using a commercial FE software COMSOL Multiphysics (Comsol AB, Stockholm, Sweden) to optimize the design parameters. This model can calculate the resonant frequencies of the circular thin plate, pipes and cavity accurately and also simulate the transducer in transmitting and receiving modes. The simulation model included the Solid Mechanics Domain to simulate the mechanical vibration of both the pipe organ backplate and the PVDF film, the Pressure Acoustic Domain to simulate the absolute pressure and coupling effect between the cavity and pipes, the Electrostatics Domain to simulate the charge migration inside the piezoelectric material, and finally a Multiphysics Model was applied to simulate the coupled boundaries between different physical domains. An air-sphere was defined to enclose the transducer to simulate its working environment. The boundary layer of the air-sphere was defined as a perfectly matching layer to make sure that sound waves can pass through the boundary without reflection as shown in Figure 4(b). Viscous damping was added to the air-domains to make the model more realistic. Acoustic wave excitation (electric signals) were introduced to vibrate the thin film to simulate the receiving or transmitting modes of the transducer. Finally, a Frequency Domain simulation evaluated the system from 15 to 70 kHz with a 0.5 kHz sampling rate.

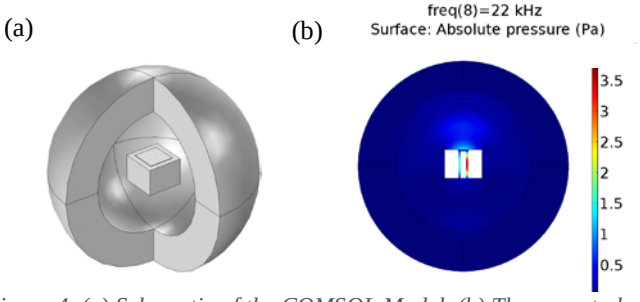

Figure 4. (a) Schematic of the COMSOL Model. (b) The x-z cut plane of a pressure plot in the cavity, pipes and the surrounding air sphere.

Part A & B investigate the resonant frequency and amplitude of the circular membrane, cavity and pipes when changing the pipes number and orientation. Part C (table 2) provides the parameters of three optimized samples which can be used in practical manufacturing.

A. *Investigating the resonance of the cavity and pipes*

The relationship between the parameters of the pipes and the absolute pressure level inside the cavity of the transducer was investigated with the COMSOL model described above. The absolute pressure level inside the cavity directly correlates with the vibration and the electric potential of the piezoelectric thin plate [19]. There are four designs (as shown in Table 1) which have different size or number of pipes for comparison: no pipe device (I) , 4 pipes devices with different pipe diameters (II) and (III) and 8 pipes device (IV). The simulated frequency spectrum is given in Figure 6 and the related pressure and displacements plot are given in Figure 5. The dashed boxes in Figure 6 from left to right represent: (a) the fundamental mode of the Helmholtz resonator, (b) the fundamental mode of the pipes, (c) the 2nd harmonic mode of the Helmholtz resonator, (d) the fundamental mode of the circular thin plate, (e) the 2nd harmonic mode of pipes, and (f) the 3rd harmonic mode of the Helmholtz resonance respectively. Three conclusions can be obtained from Figure 6:

- Designs III and IV have the same 1st (a) and 2nd (c) Helmholtz resonance because their cross-sectional area, volume of cavity and the average pipe length are equal (as shown in equation 4).
- Designs IV has more frequency spectrum fluctuations in area (b) than designs II and III because it has more pipes.
- All of the pipe organ designs (II, III, IV) have larger gain than the reference no pipe device (I) because the Helmholtz resonance can improve the overall sensitivity.

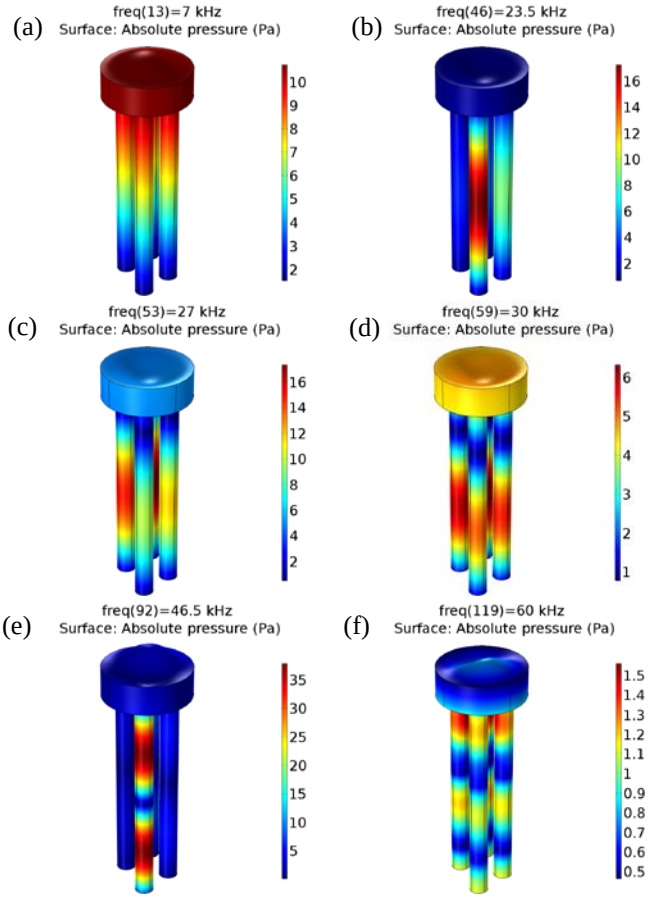

Figure 5. The pressure (different resonances) in the pipes and cavity and the vibration of the thin plate when frequency is (a) 7kHz (b) 23.5kHz (c) 27kHz, (d) 30kHz, (e) 46.5kHz, (f) 60kHz for the 4 pipes device (III), with (a)-(f) corresponding to the frequency in Figure 6

Table 1. Six designs to illustrate the coupling effect between the cavity, the multiple pipes and the circular membrane

Device	No pipe (I)	4 pipes (II)	4 pipes (III)	8 pipes (IV)	8 pipes (V)	13 pipes (VI)
Orientation pipe	n/a	No	No	No	Yes	Yes
Volume of cavity V (mm^3)	6.38	6.38	6.38	6.38	6.38	6.38
Depth of cavity h (mm)	0.97	0.97	0.97	0.97	1.45	1.45
Diameter of pipes d (mm)	n/a	0.424	0.6	0.424	0.424	0.424
Radius of cavity R (mm)	1.45	1.45	1.45	1.45	1.45	1.45
Length of pipes L (mm)	n/a	7.1, 6.8, 6.6, 6.4	7.1, 6.8, 6.6, 6.4	7.1, 7.0, 6.9, 6.8, 6.7, 6.6, 6.5, 6.4	7.1, 7.0, 6.9, 6.8, 6.7, 6.6, 6.5, 6.4	7.3, 7.2, 7.1, 7.0, 6.9, 6.8, 6.7, 6.6, 6.5, 6.4, 6.3, 6.2
Total area of the pipe S (mm^2)	n/a	0.56	1.13	1.13	1.13	1.68

.

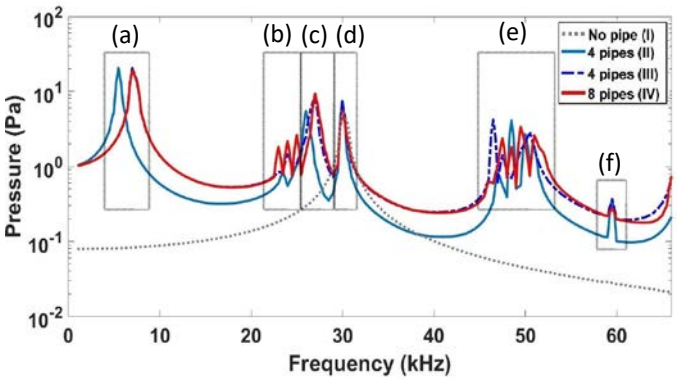

Figure 6. Absolute pressure in the cavity against frequency to investigate the number and length of pipes

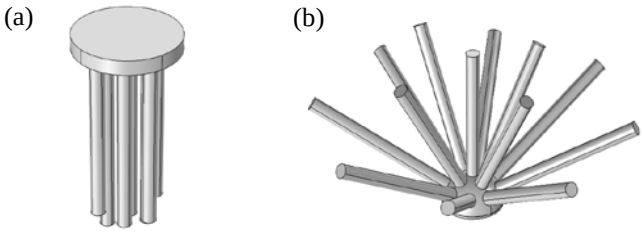

Figure 7. Air domain of the pipe organ backplate without (a) and with (b) pipe orientation.

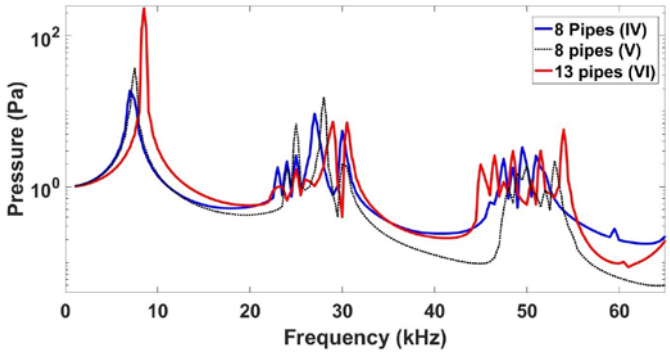

Figure 8. Absolute pressure in the cavity against frequency to investigate the orientation of pipes.

B. Investigating the orientation of the pipes

A further improved pipe organ backplate design was proposed in order to increase the number of pipes (as in Figure 7 (b)) with the same fabrication resolution, which was called the "hedgehog" design. The half-sphere cavity gives a larger surface area to accommodate more pipes and also helps the ultrasonic energy focus to the center of the thin plate. In this section, there are three designs (as shown in Table 1) for comparison: 8 pipes without orientation (IV), 8 pipes with orientation (V) and 13 pipes with orientation (VI). Two conclusions can be obtained from Figure 8:

- The "hedgehog" 13 pipes device (VI) provides the greatest Helmholtz resonance pressure, which is around 7 kHz, and the "hedgehog" 8 pipes device (V) has larger resonance pressure than the vertical 8 pipes device (IV).
- The 13 pipes "hedgehog" device (VI) gives more frequency spectra fluctuations in the pipes' 2nd harmonics than the other two devices around 50 kHz.

Table 2. Three optimized samples in practical manufacturing

Device	13 pipes	8 pipes	No pipe
Orientation pipe	Yes	No	n/a
Depth of cavity h (mm)	1.45 (half-sphere)	0.4	0.4
Diameter of pipes d (mm)	0.424	0.424	n/a
Radius of thin plate R (mm)	1.45	1.45	1.45
Length of pipes L (mm)	5.1, 5.1, 5.2, 5.3, 5.4, 5.5, 6.2, 5.5, 6.0, 6.6, 6.7, 6.9, 7.0	7.9, 7.9, 7.8, 7.7, 7.6, 7.4, 7.2, 7.2	n/a
Overall Size (mm^2)	126.7	50.2	2.46

C. Optimized samples

The parameters given in Table 1 were only used to study and quantify the resonant frequencies of the pipe organ backplate. The resonances are far away from each other in order to locate individual ones clearly. In a practical design, the resonances should be much closer to each other in order to provide more stable gain in a specific frequency range. This section provides two optimized pipe organ (vertical and hedgehog pipes) designs to compare against the standard device (as in Table 2). The extra overall size of this pipe organ transducers arise from the length of the pipes. The active areas (piezoelectric thin plate) are the same. With ongoing developments in manufacturing resolution,

it is possible to miniaturize the whole device to increase the central frequency. The normalized transmitting voltage response (TVR) and receiving voltage response (RVR) are plotted in Figure 9. The no pipe device has a very narrow bandwidth at 29 kHz, whereas the pipe organ devices have many small peaks at around 30 kHz and 55 kHz. In other words, the pipe organ transducers should have larger operating frequency ranges (wider bandwidth), which matches the 1D theoretical conclusions made by Walker and Mulholland [12]. This model only includes the air damping (but not the material damping) which makes the amplitude infinitely large at resonant frequency. Manually adding a material damping does improve the simulation result, but it will take away the possibility of easily locating the different resonant frequencies in the design stage. Therefore, the bandwidth of the transducers is not compared in the simulation section of this paper, but will be in the experimental section.

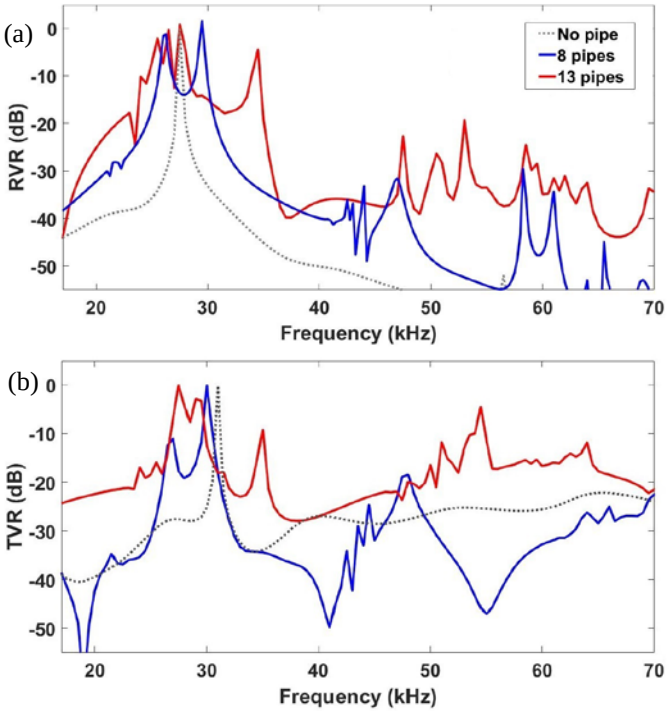

Figure 9. Simulated normalized (a) Receiving Voltage Response (RVR) and (b) Transmitting Voltage Response (TVR)

IV. Fabrication

A. Stereolithography backplates

After building a CAD model, an Asiga Pico Plus 27 additive manufacturing machine was utilized to fabricate the pipe organ backplate (see Figure 10). This is a commercial stereolithography 3D printer with 27 μm pixel resolution in the X-Y plane and ~ 1 μm in Z resolution. However, the actual print resolution is worse than this as it also depends on many other factors such as the constituents of the printer resin and the exposure time for each layer, among other things. Instead of using commercial resins directly, the improved resins [21] used in this project are prepared by mixing Polyethylene (glycol) Diacrylate (PEGDA) with molecular weight of 250 along with (2, 4, 6-trimethylbenzoyl) phenylphosphane oxide (Irgacure 819) (1% by weight) and Sudan I (0.2% by weight) vigorously in a spinner. Hua Gong et al. [21] proposed that the resins formed by this improved formula will present long-term stability in water and higher printing resolution. The exposure time is set to be 2s with a 10 μm build layer.

During manufacture, the actual printed size was found to always be smaller than the target size because of polymer shrinkage [22]. So a correction factor was required to compensate for this. First of all, calibration pipes were printed with different lengths and diameters. Secondly, a high-resolution optical microscope system was used to measure the radii. The mean value between five measurements was then calculated. Finally, the correction factor was calculated from equation (5) and the data plotted in Figure 11, with an error bar to show that when the diameter is less than 0.5mm, the correction factor dramatically decreases. In other words, a ~0.5mm diameter pipe is the smallest diameter that can be fabricated with this technology. In order to connect more pipes to the cavity, the diameter of the pipes should be as small as possible. This is the reason why $d = 0.48mm$ is chosen for this work.

$$Correction\ factor = \frac{Actual\ Diameters}{Target\ Diameters} \quad (5)$$

Figure 10. £1 coin and stereolithography pipe organ backplates for scale

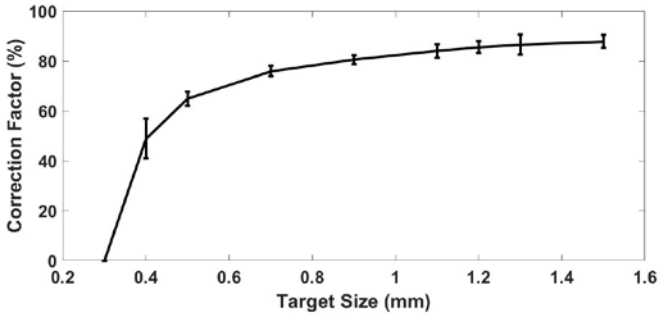

Figure 11. Correction factor against target diameter. The error bar was from five measurements.

B. PVDF thin film and circuit

Figure 12 shows a schematic illustrating the further four steps of the fabrication. The manufacture starts with (a) the additive manufactured pipe organ backplate with a gap on the side; (b) two-side-metalized PVDF film (Precision Acoustics Ltd, Dorset, UK) is attached on the top backplate with superglue; (c) the gap is filled with silver paint to connect the bottom surface of PVDF thin film. Finally, (d) a copper wire is connected to the silver gap and another one to the top surface of the film. When attaching the PVDF film with super glue, some of the super glue may enter the cavity which makes the diameter

smaller (or larger) than the designed size, and thus changes the resonance of the thin plate's flexure mode.

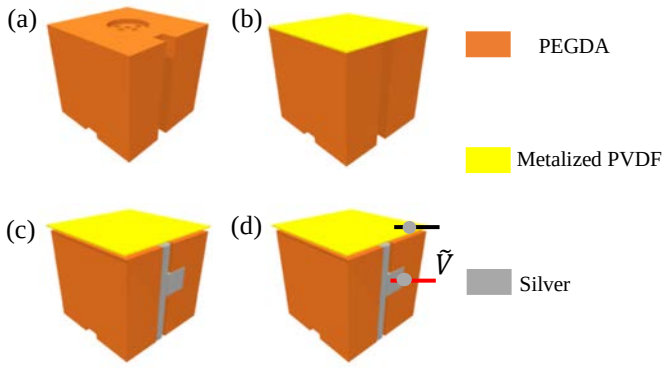

Figure 12. Four steps fabricate the pipe organ transducer (a) stereolithography pipe organ backplate. (b) Gluing metalized PVDF thin film. (c)Silver paint the gap (d) Connect copper wire to the electrode.

V. Experiment Set-up and Results

The evaluation of the pipe organ ultrasonic transducer includes measuring the vibration of the active film and the electrical signal in both time and frequency domain.

A. 3D Laser Doppler Vibrometer (LDV)

Initially, 10 V wideband periodic chirps with equal energy across frequencies from 15 to 70 kHz were generated by a signal generator to drive the active film into vibration. Secondly, the front face average displacement was obtained by a 3D LDV (MSA100-3D, Polytec, Inc., Waldbronn, Germany). Finally, the frequency spectrum and the vibration modes of the resonant frequencies were plotted (see Figure 13). From this test, the fundamental and 2nd harmonic flexure modes of the circular PVDF film between the three devices (as in Table 2) were 29 ± 3 kHz and 58 ± 6 kHz respectively (which are the same as the theoretical prediction).

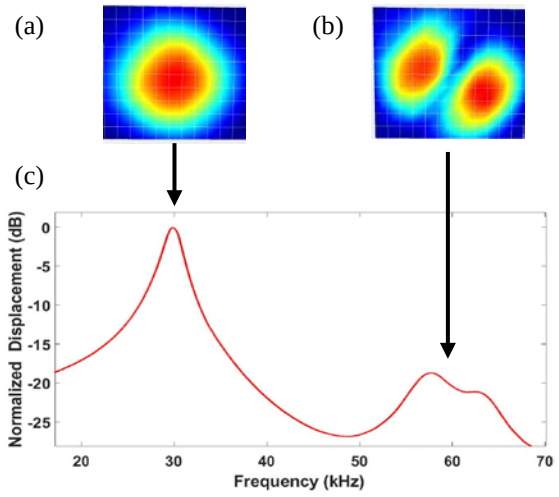

Figure 13. (a) Fundamental, (b) 2nd harmonic flexure mode of the circular PVDF film and the colors represent the displacement in the out of plane direction and (c) Average displacement spectrum of the active area measured by 3D LDV

B. Electrical signal measurement

The experimental setup for measuring the receiving and transmitting bandwidth is shown in Figure 14 (a) and (b), respectively. In Figure 14 (a), the function generator produced a 70 kHz pulse which has equal energy up to ~70 kHz to drive a broadband ultrasonic transmitter (Ultra Sound Advice Loudspeaker). The sample was far enough away from the transmitter to avoid near field effects. The electrical signal generated from the sample was amplified by a commercial charge amplifier (Brüel and Kjær type 2692) with a custom built filter (bandwidth 10-100 kHz) system, and finally acquired on an oscilloscope. A 1/8 inch reference microphone (Brüel and Kjær, Type 4138) was used to measure the reference sound pressure around the sample. The frequency response of this microphone is calibrated to be flat up to 110 kHz. An amplitude correction algorithm was utilized to compensate for the transmitter's output variance. In Figure 14(b), the function generator produced a 10V pulse to drive the film into vibration and the ultrasound field generated by the sample was measured by the reference microphone directly. Since the frequency range of our device is narrower than 110 kHz, no amplitude compensation is required. Figures 15 and 16 show the electrical signal response in TVR and RVR between the standard no pipe, 8 pipes and "hedgehog" 13 pipes devices.

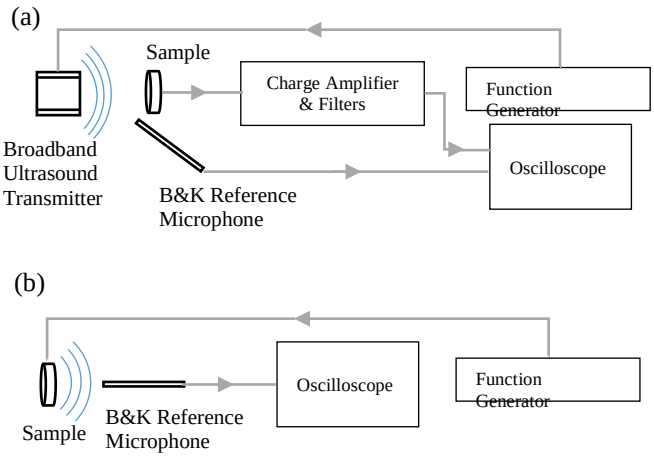

Figure 14. Simplified schematic of the experimental setup of the receiving and transmitting modes

Table 3. Experimental result of TVR and RVR.

Mode	Device	13 pipes	8 pipes	No pipe
TVR	-6 dB Bandwidth	55.7%	29.2%	12.3%
	Signal strength	0.091V	0.048V	0.106V
	Central frequency	47 kHz	27kHz	29kHz
	20% Peak-Peak Pulse length	8.8μs	20.1μs	20.5μs
RVR	-6 dB Bandwidth	58.5 %	26.0 %	9.7 %
	Signal strength	0.037 V	0.010V	0.015V
	Central frequency	41kHz	26kHz	30kHz
	20% Peak-Peak Pulse length	12.3μs	20.6μs	27μs

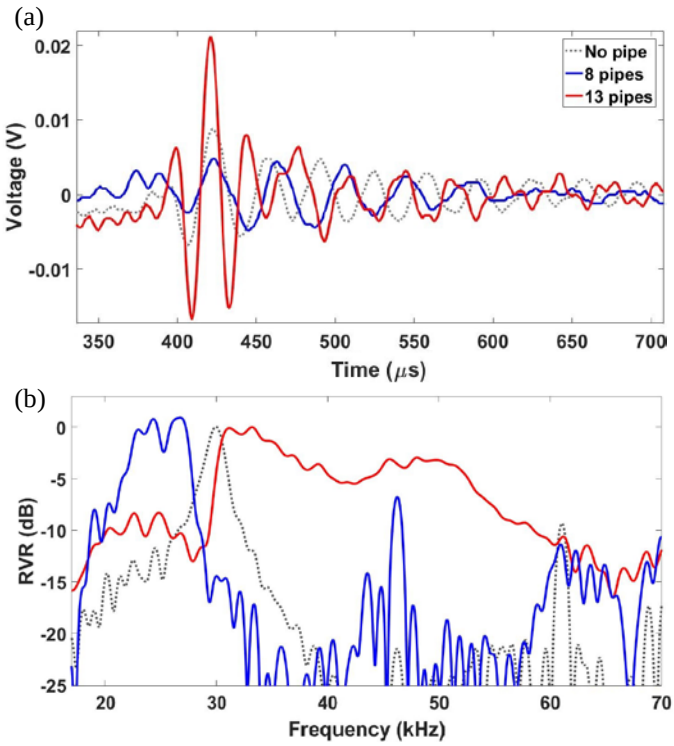

Figure 15. Receiving voltage response (RVR) in (a) time domain (b) Frequency domain

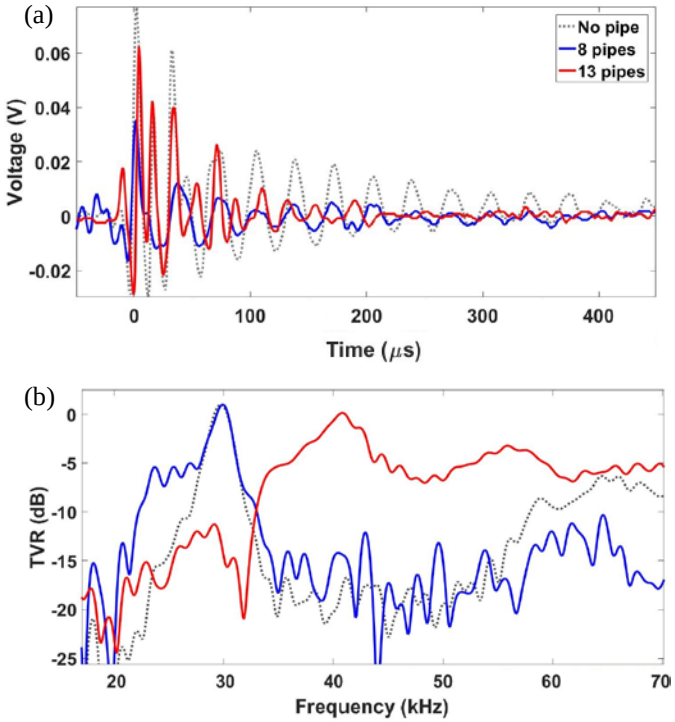

Figure 16. Transmitting voltage response (TVR) in (a) time domain (b) Frequency domain

C. Repeatability experiment

In order to prove the repeatability of the "hedgehog" 13 pipes transducer another three samples were fabricated in order to re-measure their RVR (see Figure 17). The -6 dB bandwidth of those three devices are 52.9% (not a continuous bandwidth), 50.9% and 50.9% respectively which are very close to the first 13 pipes device in Table 3 (58.5%). Moreover, their frequency spectrums are also very similar (above 25kHz) except one of the resonances was shifted at around 37 kHz. This was caused by the tolerance of fabrication when manually attaching the PVDF film with superglue.

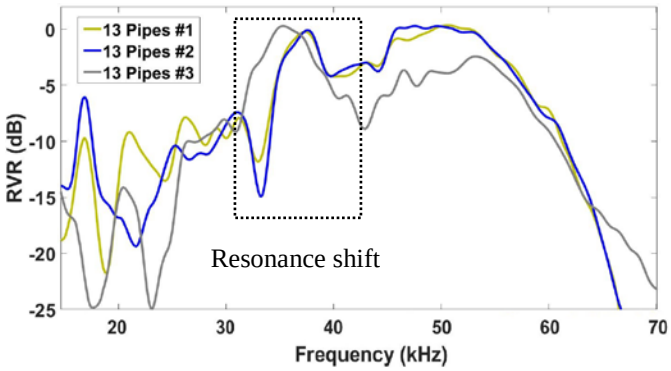

Figure 17. Repeatability experiment of three 13 pipes pipe organ transducers in RVR measurement

VI. Discussion and Conclusions

A. Simulation and Experiment Result Discussion

The pipe organ backplate is a resonator which is formed by a cavity with connecting of pipes of various length. Therefore, it includes many fundamental resonances and harmonics from those components. Section II and III evaluated those resonant frequencies from both mathematical and FEA model aspects to give the same conclusions. Section III (A) investigated the resonance of the pipes and the cavity. The simulation results, shown in Figure 6, indicate that the resonant frequency of a pipe is mainly determined by its length, which can also be explained by equation (3). Furthermore, equation (4) indicates that the resonant frequency of the Helmholtz resonator depends on the area of the opening and the cavity volume. Therefore, samples III and IV have the same Helmholtz resonant frequency in Figure 6 boxes (a) and (c). Section III (B) investigated the effect of the orientation of the pipes ("hedgehog" design). The pipes are designed to be orientated at different angles since previous 1D theoretical work concluded that the number of pipes should be as high as possible in order to have the widest bandwidth [12]. However, the number of pipes is limited by the resolution of the additive manufacturing technique in the lab. The "hedgehog" design provides a larger space to arrange the pipes because of the curved cavity surface. In other words, the "hedgehog" design increases the number of pipes with the same manufacturing resolution. Moreover, the "hedgehog" design provides additional benefits and Figures 8 and 9 show that the "hedgehog" design has a larger Helmholtz resonance and more stable gain, because the orientated pipes can focus ultrasound energy to the thin plate center.

In the optimized designs, the resonant frequencies of the cavity, multiple pipes and the circular piezoelectric film were chosen to be close to each other in order to have a flat bandwidth response in both TVR and RVR. The results in Table

3 show that the bandwidth of the pipe organ devices are at least twice as wide as that of the no pipe device with comparable sensitivity. The "hedgehog" device has the largest bandwidth and shortest pulse length in both transmitting and receiving modes. However, the disadvantage is that the "hedgehog" device also requires larger space to place the orientated pipes. The result from the 3D LDV (as shown in Figure 13) indicates that the 1st flexure mode of those three transducers is around 29 kHz, which is the same as the FEA result and the value calculated from equations (1) and (2). The FEA simulation result has sharp gain peaks which caused the simulated bandwidth to be smaller than the experimental bandwidth. This is because the model did not include any electrical or mechanical damping. However, the resonant frequencies from different components of the pipe organ backplate are a good match. The pipes' fundamental and 2nd harmonic resonance varied from 20 to 25 kHz and 45 to 55 kHz respectively, and the Helmholtz resonance was located at 35kHz to fill the gap between the pipes' resonance modes and increase the overall device sensitivity. This is why the 13 pipes pipe organ transducer can introduce a stable gain from 30 to 55 kHz in the experiment results. Although the vertical pipe design can have similar pipe lengths and cavity size, the "hedgehog" device can focus the ultrasound energy to the middle of the thin plate. Therefore, the "hedgehog" device has larger sensitivity improvement in the pipes' resonant frequencies. The repeatability experiment proved that the fabrication and the measurement stages are repeatable. All of the potential errors are from the tolerance of the fabrication.

B. Conclusions

The bandwidth of conventional PMUTs is too narrow to be used in wide-bandwidth applications [7]. This paper presented a novel backplate design (resonator) to improve the bandwidth by selecting and enhancing the frequency range of interest. The frequency range can be carefully controlled through the specific parameters of the backplate. The principles were studied via mathematical equations and FEA models. The models indicated that the pipe organ backplate introduced Helmholtz resonances and multiple pipes' resonances to the circular thin plate's resonance to increase the device bandwidth without sensitivity loss. This also provided several conclusions to locate and quantify different types of resonances in the frequency domain. Two optimised designs were selected for the fabrication stage to compare against the custom-built standard device. An additive manufacturing technique for the pipe organ backplate is introduced. It is a faster prototyping method for fabricating piezoelectric diaphragm ultrasonic transducers. An improved resin formula was used to increase the manufacture resolution of the backplate. Finally, two experiments were designed to evaluate the response of two pipe organ transducers, and a standard transducer, in both TVR and RVR. The -6dB bandwidth of the "hedgehog" 13 pipes device was found to be up to 58.5% in RVR, which was 2.25 times larger than the vertical 8 pipe device, and 6 times larger than the custom-built standard device. In the TVR the -6dB bandwidth of the "hedgehog"13 pipe's device was up to 55.7%, which was 1.9 times larger than the 8 pipes device, and 4.6 times larger than the customer-built standard device. The repeatability experiment shows that the fabrication and measurement progress are repeatable. The error originated from the manual fabrication process. With the ongoing development of additive manufacturing, some researchers [23] claim that they can use two-photon polymerization (TPP) for fabrication of three-dimensional structures with a lateral resolution below $200\ nm$. The authors latest simulation results, suggest that the overall size of the pipe organ air-coupled transducer can be miniaturized to be ~$500\ \mu m$, which will result in an operating frequency of 480 kHz, which is more applicable to applications such as NDE. Furthermore, it is possible to imagine that the fabrication could be achieved directly on a piezoelectric film to order to replace the gluing process used for this paper's prototypes.

ACKNOWLEDGMENTS

The authors would like to acknowledge Yansheng Zhang for designing and fabricating the custom-built filters for measuring the electrical signal. And also thanks to other staff and researchers at the Centre for Ultrasonic Engineering in the University of Strathclyde for their support throughout this research work. The study was supported by the Engineering and Physical Sciences Research Council (EPSRC) under grant EP/L022125/1, and by the European Research Council under the European Union's Seventh Framework Programme (FP/2007-2013) / ERC Grant Agreement n. [615030]. Dataset available: http://dx.doi.org/10.15129/fa341875-f1b1-4bfd-b052-41b965de95c4

REFERENCES

[1] H. Fang, Z. Qiu, R. L. O'Leary, A. Gachagan, and A. J. Mulholland, "Improving the operational bandwidth of a 1-3 piezoelectric composite transducer using Sierpinski Gasket fractal geometry," *IEEE Int. Ultrason. Symp. IUS*, vol. 2016–Novem, pp. 8–11, 2016.

[2] P. C. Eccardt and K. Niederer, "Micromachined ultrasound transducers with improved coupling factors from a CMOS compatible process," *Ultrasonics*, vol. 38, no. 1, pp. 774–780, 2000.

[3] Y. Qiu *et al.*, "Piezoelectric micromachined ultrasound transducer (PMUT) arrays for integrated sensing, actuation and imaging," *Sensors (Basel).*, vol. 15, no. 4, pp. 8020–8041, 2015.

[4] D. E. Dausch, J. B. Castellucci, D. R. Chou, and O. T. Von Ramm, "Theory and operation of 2-D array piezoelectric micromachined ultrasound transducers," *IEEE Trans. Ultrason. Ferroelectr. Freq. Control*, vol. 55, no. 11, pp. 2484–2492, 2008.

[5] A. Guedes, S. Shelton, R. Przybyla, I. Izyumin, B. Boser, and D. A. Horsley, "Aluminum nitride pMUT based on a flexurally-suspended membrane," *2011 16th Int. Solid-State Sensors, Actuators Microsystems Conf. TRANSDUCERS'11*, pp. 2062–2065, 2011.

[6] T. Wang, T. Kobayashi, and C. Lee, "Micromachined piezoelectric ultrasonic transducer with ultra-wide frequency bandwidth," *Appl. Phys. Lett.*, vol. 106, no. 1, pp. 6–11, 2015.

[7] P. Muralt *et al.*, "Piezoelectric micromachined ultrasonic transducers based on PZT thin films," *IEEE Trans. Ultrason. Ferroelectr. Freq. Control*, vol. 52, no. 12, pp. 2276–2288, 2005.

[8] T. Wang, R. Sawada, and C. Lee, "A piezoelectric micromachined ultrasonic transducer using piston-like membrane motion," *IEEE Electron Device Lett.*, vol. 36, no. 9, pp. 957–959, 2015.

[9] A. Hajati *et al.*, "Monolithic ultrasonic integrated circuits based on micromachined semi-ellipsoidal piezoelectric domes," *Appl. Phys. Lett.*, vol. 103, no. 20, 2013.

[10] A. J. Walker and A. J. Mulholland, "A theoretical model of an electrostatic ultrasonic transducer incorporating resonating

conduits," *IMA J. Appl. Math. (Institute Math. Its Appl.*, vol. 75, no. 5, pp. 796–810, 2010.
[11] A. J. Walker, A. J. Mulholland, E. Campbell, and G. Hayward, "A theoretical model of a new electrostatic transducer incorporating fluidic amplification," *Proc. - IEEE Ultrason. Symp.*, pp. 1409–1412, 2008.
[12] A. J. Walker and A. J. Mulholland, "A pipe organ-inspired ultrasonic transducer," *IMA J. Appl. Math. (Institute Math. Its Appl.*, no. October, pp. 1–16, 2017.
[13] E. Campbell, W. Galbraith, and G. Hayward, "A new electrostatic transducer incorporating fluidic amplification," *Proc. - IEEE Ultrason. Symp.*, vol. 1, no. 1, pp. 1445–1448, 2006.
[14] B. Zhu, B. Tiller, J. F. C. Windmill, A. J. Mulholland, and A. J. Walker, "' Pipe Organ ' Air -coupled Broad Bandwidth Transducer," in *IEEE Int. Ultrason. Symp. IUS*, 2017, pp. 6–9.
[15] F. Akasheh, T. Myers, J. D. Fraser, S. Bose, and A. Bandyopadhyay, "Development of piezoelectric micromachined ultrasonic transducers," *Sensors Actuators, A Phys.*, vol. 111, no. 2–3, pp. 275–287, 2004.
[16] M. Bao and H. Yang, "Squeeze film air damping in MEMS," *Sensors Actuators, A Phys.*, vol. 136, no. 1, pp. 3–27, 2007.
[17] J. E. Mclennan and J. Close, "A0 and A1 Studies on the Violin Using CO 2 , He , and Air / Helium Mixtures," *Acta Acust.*, vol. 89, no. April 2002, pp. 176–180, 2003.
[18] S. B. Horowitz, M. Sheplak, L. N. Cattafesta, and T. Nishida, "A MEMS acoustic energy harvester," *J. Micromechanics Microengineering*, vol. 16, no. 9, 2006.
[19] M. Jabrullah and R. A. Rahim, "Design And Simulation of MEMS Helmholtz Resonator for Acoustic Energy Harvester," pp. 505–510, 2016.
[20] H. Takahashi, A. Suzuki, E. Iwase, K. Matsumoto, and I. Shimoyama, "MEMS microphone with a micro Helmholtz resonator," *J. Micromechanics Microengineering*, vol. 22, no. 8, 2012.
[21] H. Gong, M. Beauchamp, S. Perry, A. T. Woolley, and G. P. Nordin, "Optical approach to resin formulation for 3D printed microfluidics," *RSC Adv.*, vol. 5, no. 129, pp. 106621–106632, 2015.
[22] J. Stampfl *et al.*, "Photopolymers with tunable mechanical properties processed by laser-based high-resolution stereolithography," *J. Micromechanics Microengineering*, vol. 18, no. 12, 2008.
[23] J. Serbin, A. Egbert, A. Ostendorf, and B. N. Chichkov, "Femtosecond laser-induced two-photon polymerization of inorganic – organic hybrid materials for applications in photonics," vol. 28, no. 5, pp. 301–303, 2003.

Botong Zhu received the bachelor's degree from the University of Strathclyde in 2015, where he is currently pursuing the Ph.D. degree with the Department of Electronic and Electrical Engineering. He is also a PhD student in EPSRC Centre for Doctoral Training in Quantitative NDE. His research interests are in the field of air-coupled transducer development.

Benjamin P Tiller is a Research Associate at the University of Strathclyde, in the Department of Electronics and Electrical Engineering, Glasgow, United Kingdom. He did his PhD at University of Glasgow focusing on the frequency scaling relationship of acoustic streaming in microfluidic environments. Before that he completed an MSc in Physics with Theoretical Physics at University of Nottingham. His current research interests involve developing novel 3D printed techniques that enable new sensing technologies.

Alan J. Walker is a Lecturer in Mathematics at the University of the West of Scotland. He received a B.Sc. (Hons) degree in Mathematics from the University of Strathclyde, UK, in 2003 and a Ph.D. degree in Mathematics from the University of Strathclyde, UK, in 2008. He has over ten years research experience in ultrasonics. His research interests are related to mathematical modelling of physical and biological systems.

Tony Mulholland was born in Glasgow, Scotland, UK, in 1966. He received a B.Sc. Honours degree in mathematics from the University of Glasgow in 1987, a M.Sc. degree in industrial mathematics from the University of Strathclyde in 1991, and a Ph.D. degree in mathematical biology from Glasgow Caledonian University in 1994. From 1999 he has been an academic member of staff in the Department of Mathematics and Statistics at the University of Strathclyde, where he is now a Professor and Head of the Department. He has worked with the Centre for Ultrasonic Engineering (CUE) at the University of Strathclyde since 1996 and he leads the analytical modelling activities of the center. He has published over 100 papers in applied mathematics, particularly in the modelling of ultrasonic devices and systems. He is a Fellow of the Institute of Mathematics and its Applications.

James F. C. Windmill (M'99-SM'17) is a Professor in the Department of Electronic and Electrical Engineering at the University of Strathclyde, Glasgow, United Kingdom. He received a B.Eng. degree in electronic engineering from the University of Plymouth, UK, in 1998 and a Ph.D. degree in magnetic microscopy from University of Plymouth, UK, in 2002. He joined the Centre for Ultrasonic Engineering (CUE) at the University of Strathclyde as a lecturer in 2008. He has over 18 years of research and development experience in the areas of sensors and hearing systems. His research interests are in the field of biologically-inspired acoustic systems, from the fundamental biology to various engineering application topics.